

# LATERAL PRESSURES IN BOTTOM-UNLOADING SILOS BY NUMERICAL METHODS

J. C. Jofriet

*School of Engineering, University of Guelph, Guelph, Ontario N1G 2W1*

Received 8 July 1985, accepted 25 October 1985

**Jofriet, J. C.** 1986. Lateral pressures in bottom-unloading silos by numerical methods. *Can. Agric. Eng.* 28: 51-59.

Bottom-unloading farm tower silos used for the storage of haylage are subjected to very high lateral pressures at the level of the unloader. The cause of this pressure "bulge" at the unloader is the arch reaction over the unloader cavity. The finite element method of analysis has been used to quantify the high lateral pressures in the unloader zone. This paper presents the results of a number of analyses carried out to complement Dickinson's (1982) work on this topic. The present work concentrates on the effect of moisture content as it changes the weight of the material, and on the effect of the silo aspect ratio, height over diameter. The nondimensionalized lateral pressure results are shown to be affected only by the wall friction, the pressure ratio and the aspect ratio. Recommendations for a lateral pressure design curve are included in the paper.

## INTRODUCTION

Bottom-unloading oxygen-limited farm silos appear to occupy an increasing share of the overall farm silo construction volume. This type of silo allows a more automated feed-handling system than do most top-unloading silos. As well, the first-in first-out feature allows for a more or less continuous feed storage system.

At present, bottom-unloading silos are used mainly for the storage of high-moisture corn or of legumes, or legume-grass mixtures. With the latter the unloading equipment causes a cavity to form in the bottom of the silo as the rotating unloading auger moves material to the centrally located unloading hopper. The large cohesive strength of the whole-plant material allows a dome-like cavity to form which collapses at discrete intervals when arch support becomes inadequate.

Arching of the silage causes very high radial pressures where the arch intersects the silo wall. This is near the floor in the case of a "sweep-arm" type unloader (see Fig. 1) or some distance above the floor if a flail-type unloader is used.

Mahmoud (1972) was the first to provide a qualitative assessment of the wall pressure "bulge" at the level of the bottom-unloading equipment. Mahmoud also carried out quantitative work on wall pressures for bottom-unloading silos. This work was undertaken for the International Silo Association (ISA) in preparation of the present ISA Standards for the design of bottom-unloading silos (International Silo Association 1981a, b). At about the same time Dickinson (1982) carried out an extensive parametric numerical investigation of a body of haylage in a bottom-unloading silo. The effect of cavity shape, wall friction and pressure ratio were investigated in finite element analyses of a  $6 \times 20$ -m-

high body of silage having an average density of  $471 \text{ kg/m}^3$ . Design recommendations were made on the basis of these analyses (Dickinson and Jofriet 1984).

This paper presents the numerical results of an investigation that followed

Dickinson's (1982) work and that had as its three objectives: (1) to look at the effect of silo geometry on the wall pressures in a bottom-unloading silo; (2) to investigate the effect of the mass density of the silage; and (3) to explore the possibility of pre-

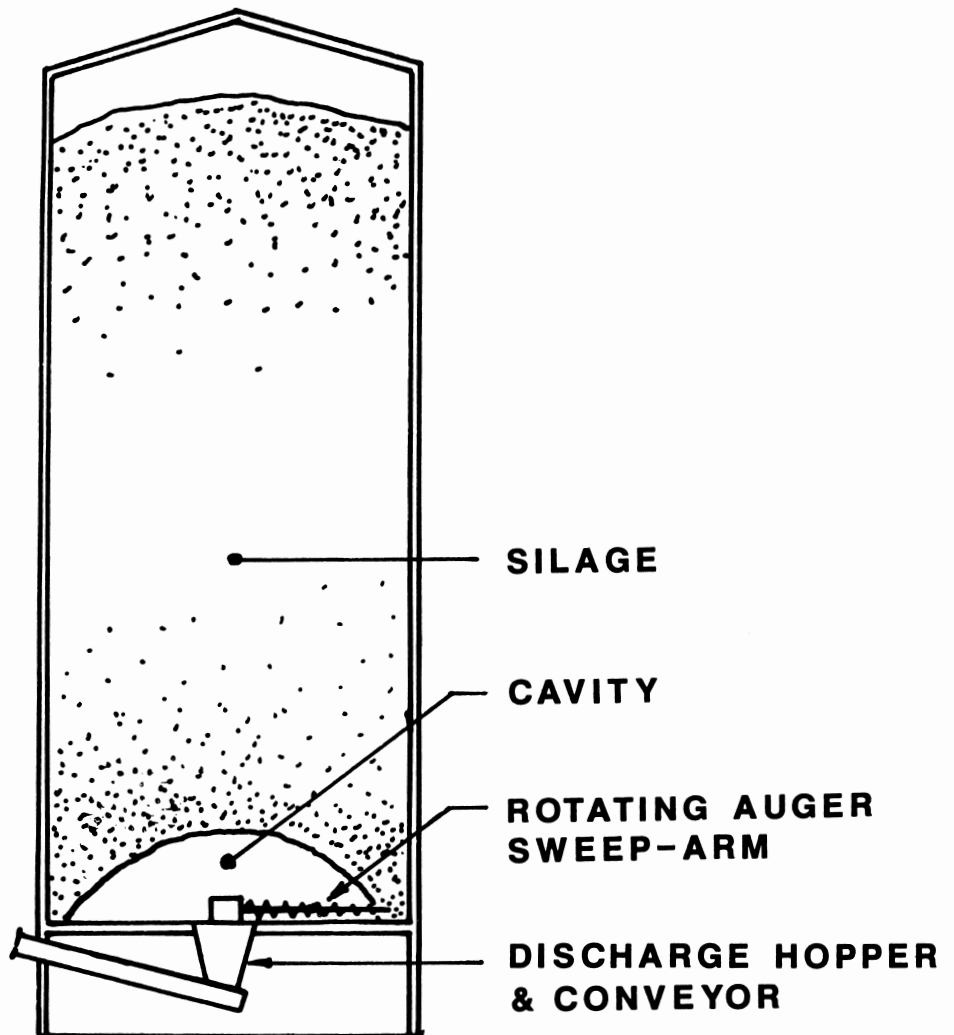


Figure 1. Auger "sweep-arm" unloader.

senting wall pressures in nondimensional form as was done for top-unloading silos (Jofriet and Czajkowski 1980).

### METHOD OF ANALYSIS

Six finite element stress analyses were carried out in addition to those done earlier by Dickinson (1982). The analyses employed nine-noded isoparametric elements in an axisymmetric stress formulation. The cylindrical boundary was assumed rigid in the radial direction. Frictional boundary forces are included in the formulation (Jofriet et al. 1977).

All analyses had 72 elements and 325 nodes. The concentration of nodes was very high in the lower region of continuum whereas few nodes were used in the upper region (Fig. 2). Indeed, the 30 elements above the horizontal plane through nodes 183 and 195 had an aspect ratio of 7.5 for the  $6 \times 25$ -m continuum of Analysis V which is borderline for this element to maintain numerical accuracy. However, the results in the upper region were of little interest for this investigation. In the important lower region the element aspect ratios are close to ideal.

Complete details of the variable parameters used in the six analyses are listed in Table I. These include the height and diameter of the silage mass, the ratio of the wall friction-force to the lateral wall force (referred to as friction coefficient) and the density of the elements. These densities were obtained using a pressure-density model for 60% moisture content alfalfa haylage (Jofriet et al. 1982) in a lamina analysis. The pressure ratio was not varied and a value of 0.5 was used throughout. The largest diameter of the dome-shaped cavity was in all cases 0.83 times the silage mass diameter, i.e. the radial position of node 11 was 2.5 m and 3.125 m for the 6.0- and 7.5-m diameters, respectively.

The purpose of analyses I and II was to compare the present wall pressure findings with those by Dickinson (1982) who used 45% moisture content alfalfa haylage exclusively. The average weight density used was  $4.71 \text{ kN/m}^3$ , 60–65% of the present average densities. It was hypothesized that if the pressures were normalized with respect to the average weight density, the wall pressures would be the same for the light and the heavier materials. The object of analyses III and IV was to expand on the single silo size that Dickinson had investigated. It was hypothesized that the pressures would be independent of size of silage mass if the wall pressures were normalized with respect to the height. The variable then becomes aspect ratio ( $H/D$ ) which is kept the same in analyses III and

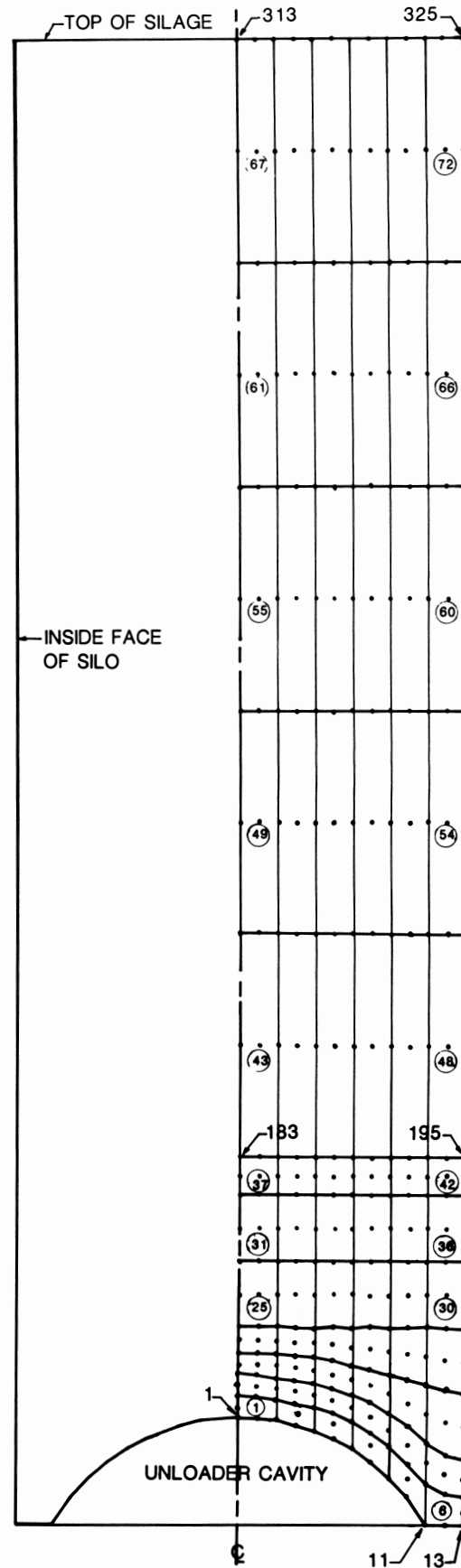


Figure 2. Node and element layout used in the finite element analyses.

IV while changing the size.

Finally, analyses V and VI were carried out to explore other values of aspect ratio. With these last two tests only one value of friction coefficient (0.5) is used.

## RESULTS

One of the main purposes of the analyses reported herein was to cast Dickinson's (1982) findings in a more general form. Jofriet and Czajkowski (1980) found that static wall pressures in a cylindrical silo are a function of the height of silage,  $H$ , the average weight density,  $\rho_{av}g$ , the aspect ratio of the silage mass,  $H/D$ , and of the product of wall friction coefficient and pressure ratio,  $\mu K$ . This is also reflected in the Janssen (1895) formula for the average vertical stress  $q$

$$q = \frac{\rho g D}{4\mu K} \left(1 - e^{-\frac{4\mu K}{D} z}\right) \quad (1)$$

in which  $z$  is the depth below top of silage and  $\rho$  the mass density of the material. We can rewrite Eq. 1 as follows

$$\frac{q}{\rho g H} = \frac{D}{4\mu K H} \left(1 - e^{-\frac{4\mu K H}{D} \frac{z}{H}}\right) \quad (2)$$

Now replacing  $q/\rho g H$  with the nondimensional average vertical pressure  $\bar{q}$ , the aspect ratio  $H/D$  with  $R$  and the ratio  $z/H$  with  $\bar{z}$  we get:

$$\bar{q} = \frac{1}{4\mu K R} \left(1 - e^{-4\mu K R \bar{z}}\right) \quad (3)$$

and the horizontal pressure

$$\bar{p} = K \bar{q}$$

In the present analyses the mass density varies with depth and in all cases the wall pressures  $p$  will be nondimensionalized by division by  $\rho_{av}gH$ . They will be plotted versus  $\bar{z}$ , or more precisely  $h/H$  where  $h$  is the height measured from the bottom,  $H-z$ .

In Figs. 3 and 4 the wall pressure results from analyses I and II are compared with the results from two analyses reported by Dickinson (1982) with exactly the same parameters except the weight of the material which was modelled as a 45% moisture content haylage with average weight density of  $4.71 \text{ kN/m}^3$ . Figure 3 has two analyses with a friction coefficient of 0.5 and Fig. 4 with 0.3.

The results of the comparable nondimensionalized pressures are extremely close and it was necessary to plot the present results and the Dickinson ones with a 0.1 offset. The Dickinson results relate to the bottom scale in Figs. 3 and 4, the present results to the top scale.

TABLE I. VALUES OF THE VARIABLE PARAMETERS IN FINITE ELEMENT ANALYSES I TO VI

Analysis	I	II	III	IV	V	VI
Silage mass height (m)	20	20	25	25	25	20
Silage mass diameter (m)	6.0	6.0	7.5	7.5	6.0	7.5
Friction coef.	0.5	0.3	0.5	0.3	0.5	0.5
Weight density of silage ( $\text{kN/m}^3$ )						
Elements 1-30†	8.64	9.74	9.47	10.30	8.85	9.19
Elements 31-36	8.48	9.54	9.33	10.18	8.75	9.01
Elements 37-42	8.42	9.45	9.27	10.12	8.70	8.96
Elements 43-48	8.23	9.20	9.10	9.93	8.56	8.71
Elements 49-54	7.78	8.59	8.66	9.42	8.18	8.18
Elements 55-60	7.08	7.67	7.91	8.52	7.55	7.37
Elements 61-66	6.03	6.31	6.67	7.00	6.47	6.16
Elements 67-72	4.47	4.51	4.73	4.77	4.70	4.50
Average	7.24	7.93	7.96	8.57	7.57	7.58

† Element numbers are identified in Fig. 2.

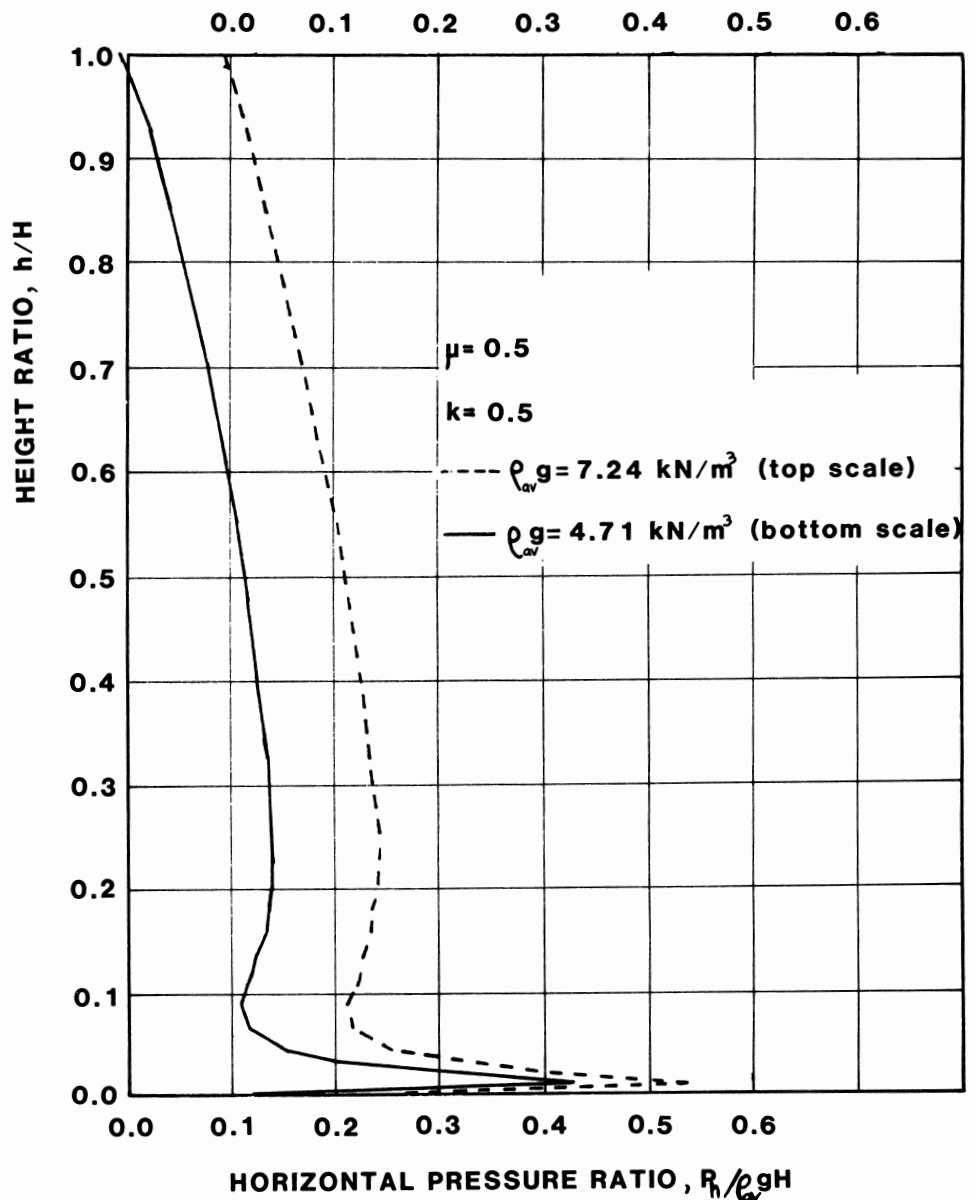
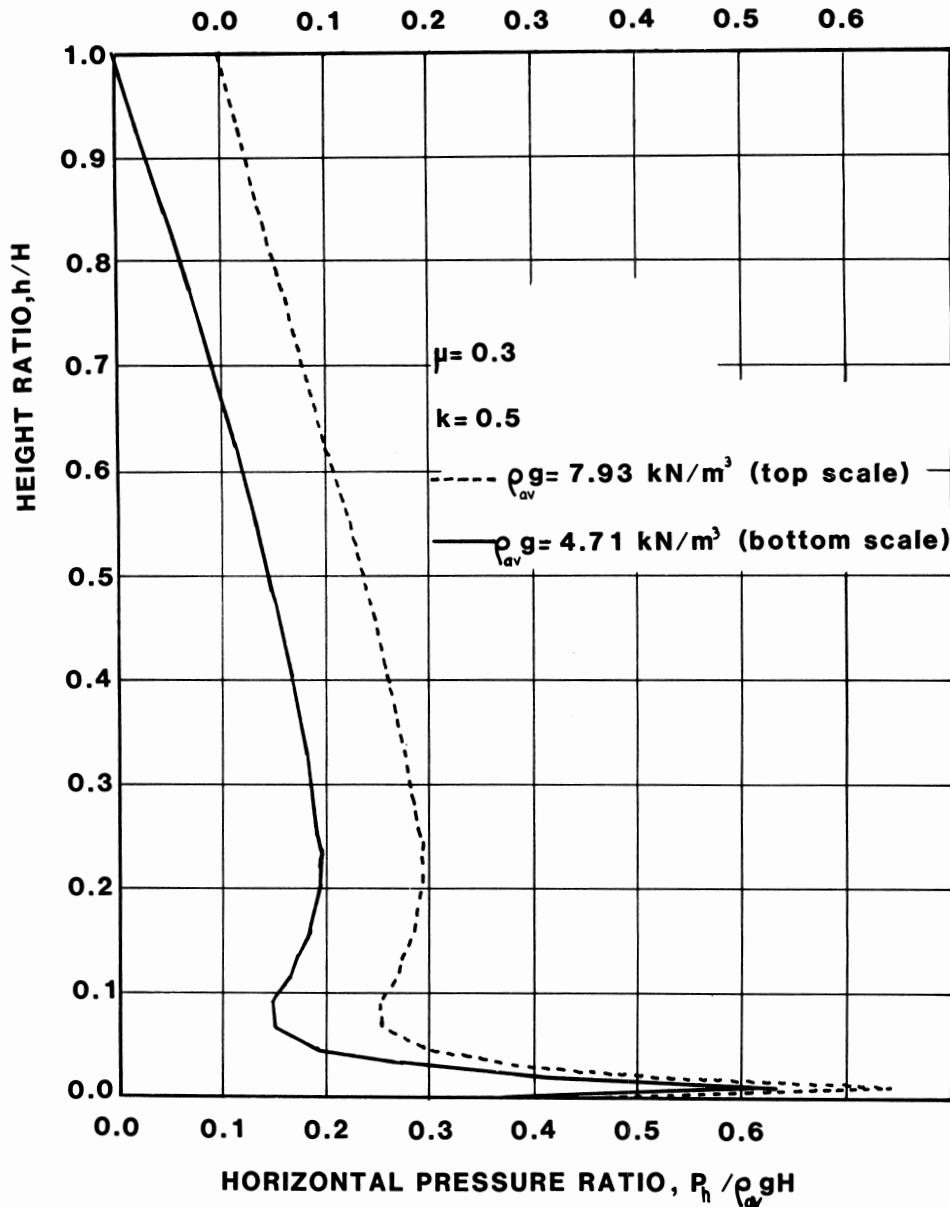


Figure 3. Nondimensionalized horizontal pressures vs. height for 45% and 60% alfalfa silage (average weight  $4.71$  and  $7.24 \text{ kN/m}^3$  respectively);  $\mu = 0.5$  and  $K = 0.5$ .



**Figure 4.** Nondimensionalized horizontal pressures vs. height for 45% and 60% alfalfa silage (average weight 4.71 and 7.93 kN/m<sup>3</sup> respectively);  $\mu = 0.3$  and  $K = 0.5$ .

Figures 5 and 6 present nondimensionalized wall pressure curves for silage of differing geometry but equal aspect ratio. Figure 5 shows the results from analyses I and III both having the same friction coefficients,  $\mu$ , and the same aspect ratio,  $R$ . Similarly, Fig. 6 illustrates the results from analyses II and IV in which the friction coefficient was 0.3 and the aspect ratio 3.33. Again the wall pressures  $\bar{p}$  are very similar and it was again necessary to offset the curves 0.1. Finally, Fig. 7 presents the nondimensionalized wall pressures of analyses I, V and VI to provide a direct comparison of the effect of aspect ratio.

#### DISCUSSION OF RESULTS

A comparison of the two wall pressure curves in Fig. 3, and also in Fig. 4, shows

clearly that the finite element results from Dickinson's work can be extrapolated linearly for use of materials with higher moisture content and thus greater weight. This is not all that surprising in the upper regions of the silage body where Eq. 3 is applicable. In the lower region where the stress patterns are far from uniform the values at the stress concentration just above the floor are less predictable.

It should be borne in mind that the geometry of the cavity formed by the unloading equipment was assumed to be the same in the present analyses. Dickinson's work showed clearly that the peak pressures are a function mainly of the width of the contact area between the silage and the silo floor. The narrower this ring of contact becomes the greater the peak pressures are theoretically. In the

present analysis the width of the contact area was 1/12 the silo diameter resulting in a peak wall pressure  $\bar{p} = 0.44$  for  $\mu = 0.5$  (Fig. 3) and  $\bar{p} = 0.64$  for  $\mu = 0.3$  (Fig. 4).

The two curves in Fig. 5 in which the pressures were determined from Analyses I and III are very similar in every respect even in the region of the bottom cavity. This despite the fact that the silage masses in the two analyses are different in size and have different average densities. However, the three ratios in Eq. 3,  $\mu$ ,  $K$  and the aspect ratio  $R$  are equal in Analyses I and III. The same is true for Analyses II and IV and the nondimensionalized horizontal pressures from these analyses prove to be very similar (Fig. 6). Again, it would seem that the determining variables governing the stress behavior in the upper uniform region of the silage mass also govern the

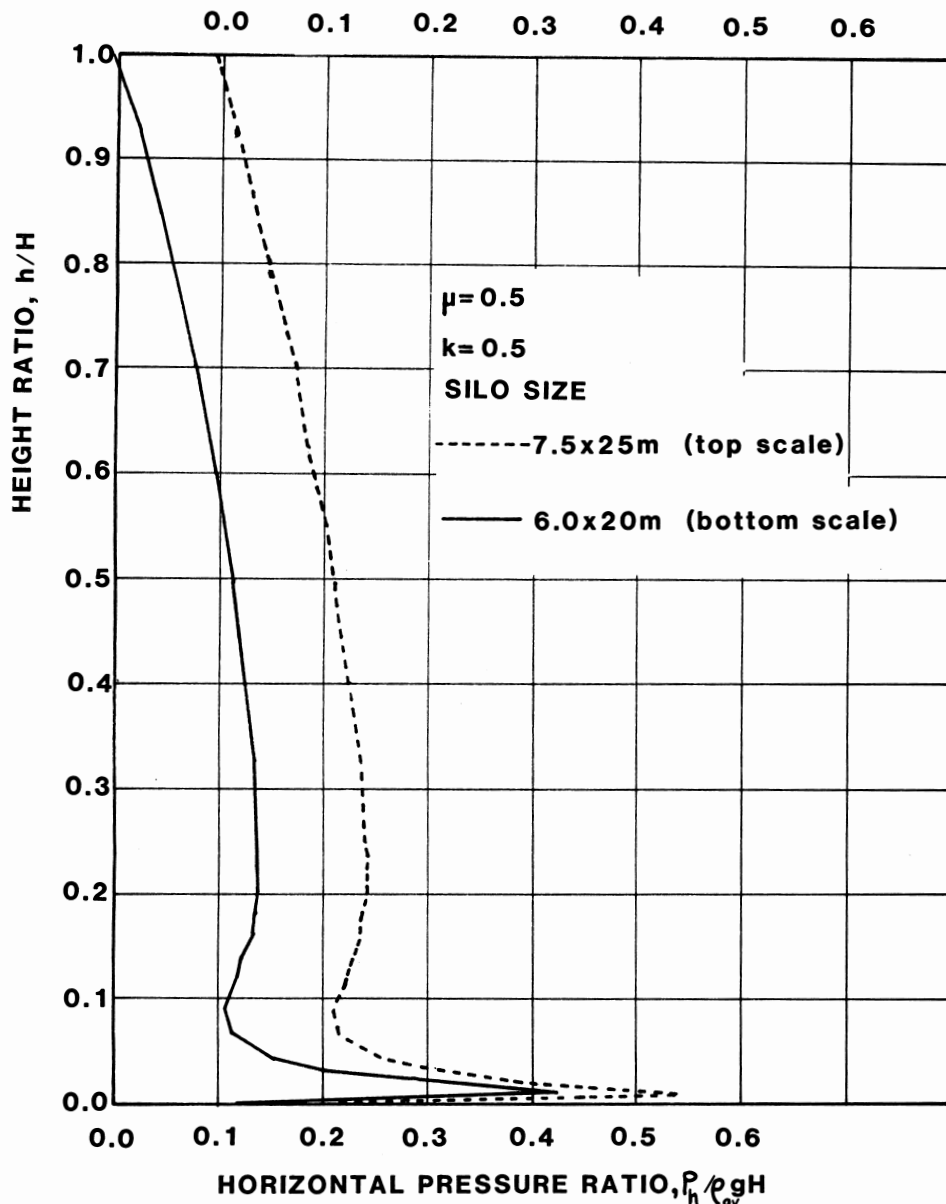


Figure 5. Nondimensionalized horizontal pressures vs. height for 60% alfalfa silage in 6 × 20-m and 7.5 × 25-m tower silos;  $\mu = 0.5$  and  $K = 0.5$ .

stresses in the lower part.

The effect of the friction coefficient can be observed by comparing the curves in Fig. 3 with those in Fig. 4. With a friction coefficient of 0.5 the peak value of  $\bar{p}$  is 0.44 whereas with a value of 0.3 this value is about 45% greater. The same can, of course, be observed by comparing Figs. 5 and 6. The general effect of  $\mu$  and  $K$  on lateral pressures in a cylindrical silo were discussed at length by Jofriet and Czajkowski (1980).

The effect of the aspect ratio  $R$  appears to be more pronounced in the cavity region than in the rest of the silo (Fig. 7). Greater aspect ratios lead to smaller pressures because of the increased influence of the wall friction reducing the vertical stress in the silage body, e.g. the wall carries a larger percentage of the weight of the silage at

every level. The peak values of nondimensionalized wall pressure are roughly linear with  $1/R$ . For  $\mu = 0.5$  the relationship is approximately

$$\bar{p} = 1.45/R \quad (5)$$

and for  $\mu = 0.3$

$$\bar{p} = 2.1/R \quad (6)$$

#### CONCLUSIONS AND RECOMMENDATIONS

The major conclusion of this paper is that wall pressures in the unloader region of a bottom-unloading silo are linear with the average weight density of the silage mass and with its height. It is possible therefore to use for design a limited number of design curves and apply them to various sizes of silo and to materials of

differing density.

The independent variables that have an effect on the values of the nondimensionalized wall pressures are the friction coefficient,  $\mu$ , the pressure ratio,  $K$ , and the silage body aspect ratio,  $R$ . This then is very similar to the behavior of a uniform material in an infinitely long cylindrical container as indicated by the nondimensional form of the Janssen equation (Eq. 3). It may be concluded then that the design recommendations made by Dickinson and Jofriet (1984) have general application if supported by experimental findings.

The magnitude of the peak horizontal pressure is inversely related to the friction coefficient  $\mu$  and the aspect ratio  $R$ . The inverse relationship with  $R$  is approximately linear as expressed in Eqs. 5 and 6.

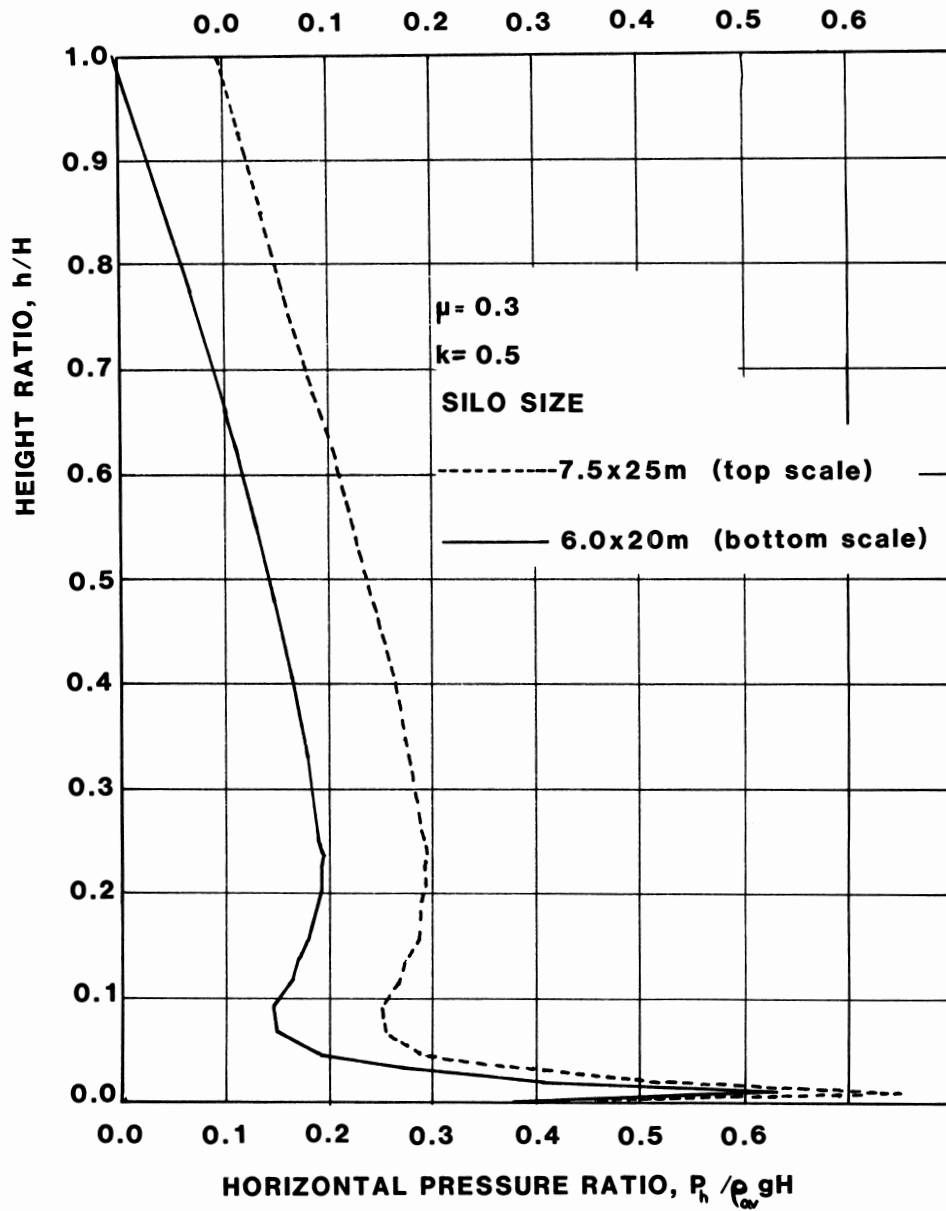


**Figure 6.** Nondimensionalized horizontal pressures vs. height for 60% alfalfa silage in 6 × 20-m and 7.5 × 25-m tower silos;  $\mu = 0.3$  and  $K = 0.5$ .

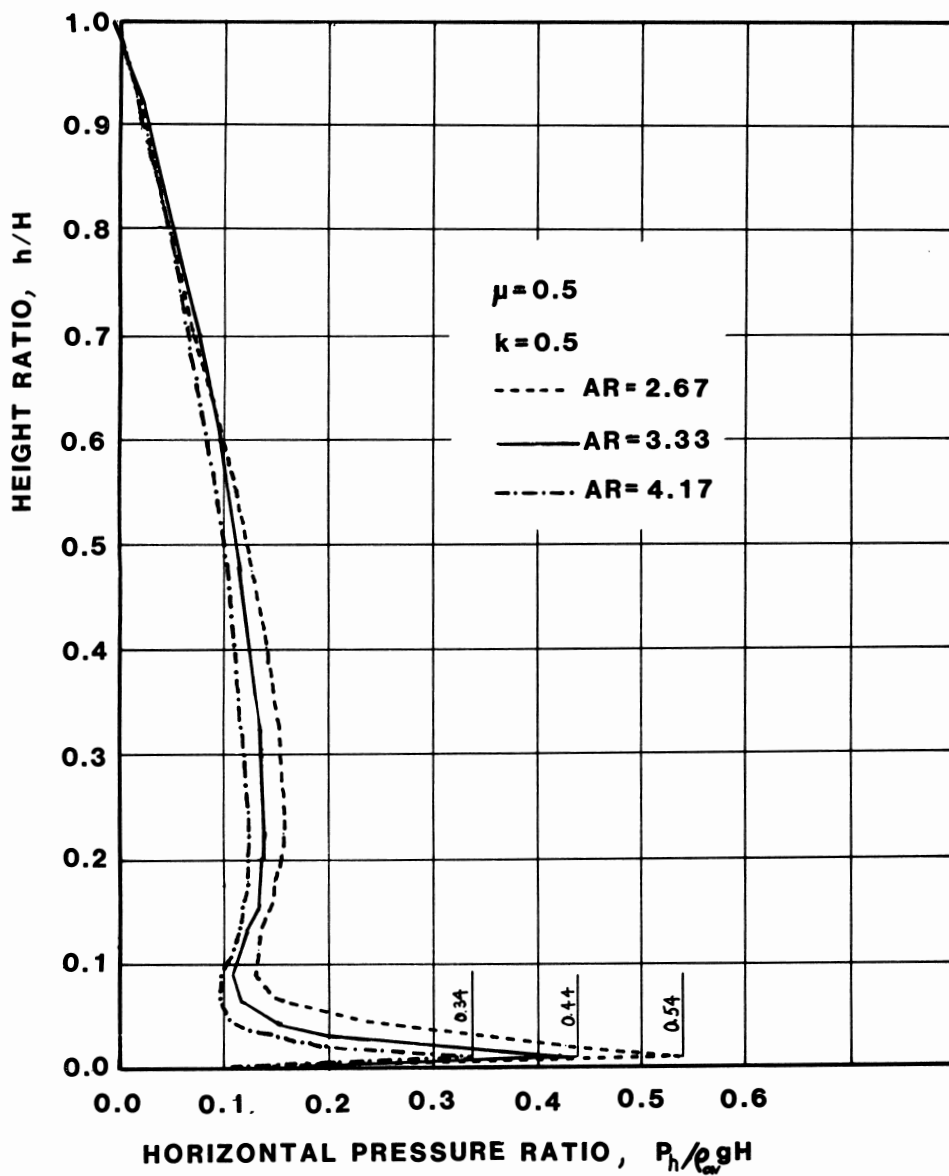


Figure 7. Nondimensionalized horizontal pressures vs. height for 60% alfalfa silage in tower silos with aspect ratios 2.67, 3.33 and 4.17;  $\mu = 0.5$  and  $K = 0.5$ .

Dickinson (1982) previously reported that the effect of  $K$  on the peak horizontal pressure is small. Reductions in  $K$  led to small reductions in pressure.

In view of the conclusion that the earlier design recommendations by Dickinson and Jofriet (1984) have general application they will be included here with a slight modification. They are an extension of earlier recommendations by Jofriet (1980) for top-unloading silos. The extensions include a higher-than-normal pressure at the bottom to account for the unloader cavity and an impact factor which varies linearly from 1 at mid-height to 1.25 at the silo bottom.

Dickinson and Jofriet (1984) suggested a concentrated horizontal reaction to arching over the unloader cavity of  $0.19q_1D$  per unit length of circumference at the level of the unloading equipment. This includes an impact factor of 1.25. They also suggested that this reaction be distributed over a height of  $D/5$  to provide a design pressure over that height of  $0.95q_1$  in which  $q_1$  is the average vertical pressure in the silo at the bottom.

In view of the present results (e.g. Fig. 7) a distribution over a height of  $D/6$  appears more appropriate and thus the higher-than-normal wall pressure caused by the bottom-unloading equipment should be designed for by a uniformly distributed pressure of  $0.19q_1D/(D/6) = 1.2q_1$  over a height of  $D/6$ .

Thus, the present recommendations are:

$$p_d = (2p_{1/2}/H)z \quad \text{for } 0 < z < H/2$$

$$p_d = ((2.5p_1 - 2p_{1/2})/H)z + 2p_{1/2} - 1.25p_1 \quad \text{for } H/2 < z < (H - D/6) \quad (7)$$

$$p_d = 1.2q_1 \quad \text{for } (H - D/6) < z < H$$

where  $p_d$  are design pressures,  $p_{1/2} = Kq_{1/2}$ ,  $p_1 = Kq_1$ ,  $q_{1/2}$  is  $q$  determined with the Janssen equation (Eq. 1) for  $z = H/2$  and  $\rho = \rho_{av}$  and  $q_1$  for  $z = H$  and  $\rho = 1.2\rho_{av}$ . Figure 8 shows a sample design curve; the Appendix contains the calculations for this curve. It should be realized that even this increased design pressure at the unloader of  $1.2q_1$  will not be larger than the peak pressure that will occur at any time. However, the integral over the height  $D/6$  will be more than adequate to represent the peak force that might be expected to occur. A final recommendation is that the above design recommendations be checked again against experimental results of full-scale wall pressure measurements now underway at Guelph. Preliminary findings indicate good agreement of numerical results with experiments.

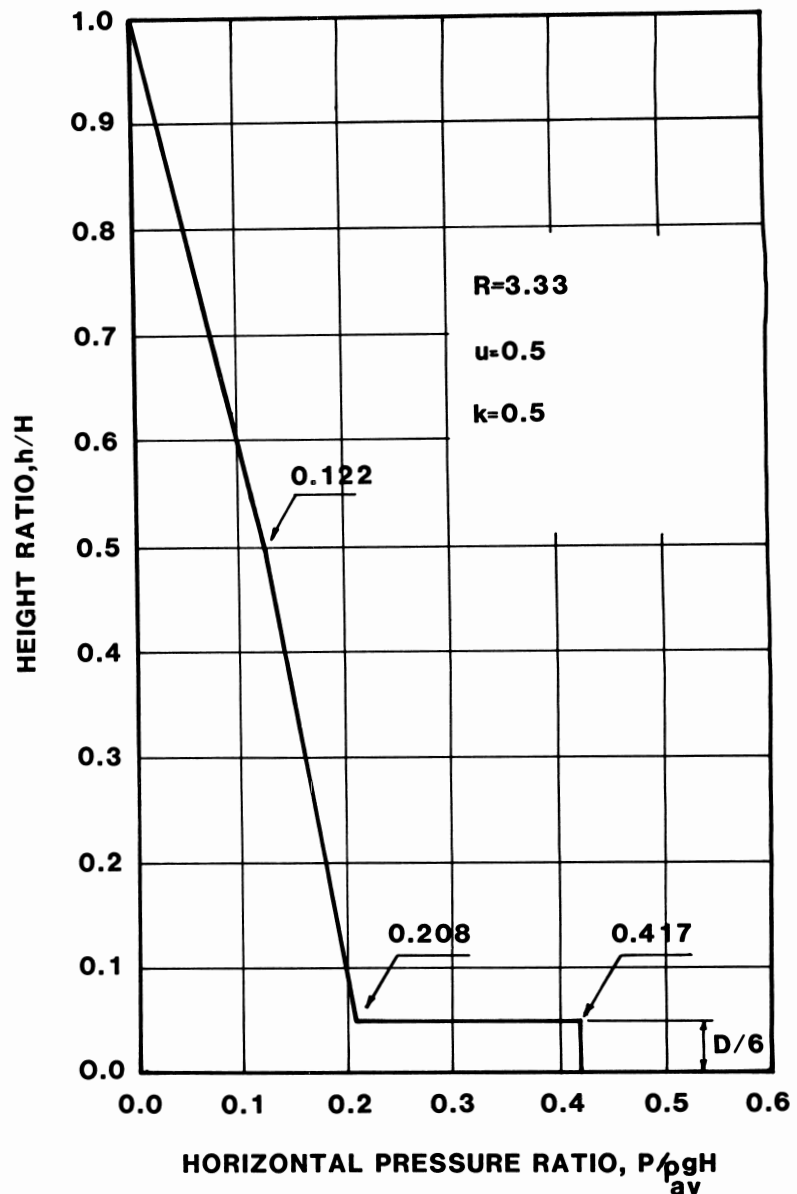


Figure 8. Proposed horizontal pressure design curve for a bottom-unloading silo with aspect ratio 3.33,  $\mu = 0.5$  and  $K = 0.5$ .

#### ACKNOWLEDGEMENTS

The work reported herein was carried out with the financial assistance of the Natural Sciences and Engineering Research Council of Canada through an operating grant.

#### REFERENCES

- DICKINSON, R. R. 1982. The functional and structural design of bottom-unloading silage silos. M.Sc. thesis, School of Engineering, University of Guelph, Guelph, Ontario.
- DICKINSON, R. R. and J. C. JOFRIET. 1984. Wall pressures in bottom-unloading farm silos. *J. Am. Conc. Inst.* **81**(2): 61-68.
- INTERNATIONAL SILO ASSOCIATION. 1981a. Recommended practice for the design and construction of atmosphere controlled bottom-unloading stave concrete farm silos. ISA Inc., Des Moines, Iowa.
- INTERNATIONAL SILO ASSOCIATION. 1981b. ISA recommended practice for the design of atmosphere controlled bottom-unloading monolithic concrete farm silos. ISA Inc., Des Moines, Iowa.
- JANSEN, H. A. 1895. Versuche uber Getreidedruck in silozellen. *V.D.I.* **19**: 1045-1049.
- JOFRIET, J. C., B. LELIEVRE, and T. F. FWA. 1977. Friction model for finite element analyses of silo. *Trans. ASA (Am. Soc. Agric. Eng.)* **20**(4): 735-740, 744.
- JOFRIET, J. C. and J. CZAJKOWSKI. 1980. A parametric study of whole-plant corn silage pressures and loads in tower silos. *Can. Agric. Eng.* **22**(1): 1-7.
- JOFRIET, J. C., P. SHAPTON, and T. B. DAYNARD. 1982. Haylage densities, pressures, and capacities in tower silos. *Can. Agric. Eng.* **24**(2): 141-148.
- MAHMOUD, M. H. 1972. Bottom-unloading silos — structural design considerations. National Silo Assoc. 60th Annual Convention; *Silo Structures — Pressure and Design*, Minneapolis, Minn. pp 62-80.

## APPENDIX

Example calculations for design curve shown in Fig. 8.

Silo  $6 \times 20$  m;  $\mu = 0.5$ ;  $K = 0.5$ ;  $\rho_{\text{avg}} = 7.24 \text{ kN/m}^3$

Thus,  $R = H/D = 3.33$  and  $4\mu K = 1$

By Eq. 1:

$$q_{1/2} = \frac{7.24 \times 6}{1} \left(1 - e^{-\frac{1 \times 10}{6}}\right) = 35.2 \text{ kN/m}^2$$

$$\bar{q}_{1/2} = q/\rho_{\text{avg}}gH = 35.2/(7.24 \times 20) = 0.243$$

$$q_1 = \frac{1.2 \times 7.24 \times 6}{1} \left(1 - e^{-\frac{1 \times 20}{6}}\right) = 50.3 \text{ kN/m}^2$$

$$\bar{q}_1 = 50.3/(7.24 \times 20) = 0.347$$

By Eq. 7:

$$\text{for } 0 < z < 10 \quad p_d = \frac{2 \times 0.5 \times 35.2}{20} z = 1.762z$$

$$\text{at } z = 10 \text{ m} \quad p_d = 17.62 \text{ kN/m}^2 \text{ and } \bar{p}_d = 0.122$$

for  $10 < z < 19$

$$p_d = \frac{2.5 \times 0.5 \times 50.3 - 2 \times 0.5 \times 35.2}{20} z + 2 \times 0.5 \times 35.2 - 1.25 \times 0.5 \times 50.3 = 1.38z + 3.82$$

$$\text{at } z = 10 \text{ m} \quad p_d = 17.62 \text{ kN/m}^2 \text{ and } \bar{p}_d = 0.122$$

$$\text{at } z = 19 \text{ m} \quad p_d = 30.04 \text{ kN/m}^2 \text{ and } \bar{p}_d = 0.208$$

$$\text{for } 19 < z < 20 \quad p_d = 1.2 \times 50.3 = 60.4 \text{ kN/m}^2 \text{ and } \bar{p}_d = 0.417$$